Research Article | Vol. 10, No. 6 | 1 Jun 2019 | BIOMEDICAL OPTICS EXPRESS 2942
Biomedical Optics EXPRESS

Terahertz spectroscopy of human skin tissue models with different melanin content

XOMALIN G. PERALTA,[1,2,*] DAWN LIPSCOMB,[3] GERALD J. WILMINK,[2] AND IBTISSAM ECHCHGADDA[2]

[1]*National Academy of Sciences NRC Senior Research Associateship, 4141 Petroleum Road, JBSA Fort Sam Houston, Texas 78234, USA*
[2]*Air Force Research Laboratory, 711th Human Performance Wing, Airmen Systems Directorate, Bioeffects Division, Radio Frequency Bioeffects Branch, 4141 Petroleum Road, JBSA Fort Sam Houston, Texas 78234, USA*
[3]*Consortium Research Fellows Program, 4141 Petroleum Road, JBSA Fort Sam Houston, Texas 78234, USA*
[*]*xomalin.peralta@gmail.com*

Abstract: Terahertz imaging has been proposed for burns and skin cancer identification. However, the role of melanocytes, melanosomes, melanin content and distribution in determining the terahertz optical properties of human skin has not been investigated. We use terahertz time domain spectroscopy to measure the optical properties of *in vitro* pigmented human skin tissue models from Asian, Black, and Caucasian donors. Spectra were collected at various time intervals and used to extract the absorption coefficient and index of refraction at terahertz frequencies. Our results indicate that the degree of cell differentiation and type of donor both contribute to the measured terahertz optical properties.

1. Introduction

The terahertz (THz) region of the electromagnetic spectrum is located between the infrared and microwave regions, spanning frequencies from 0.1 to 10 THz (wavelengths from 3000 to 30 μm). THz based applications, such as THz spectroscopy and imaging, have been proposed for the evaluation of superficial skin tissue including for the detection and diagnosis of skin burns [1–6] and cancers [7–11] as well as for the evaluation of skin absorption of drugs [12]. The effect of THz radiation on skin tissues and cells have also been investigated for wound healing response [13], skin cancer and psoriasis [14], and cell adhesion, proliferation and differentiation [15–17]. In order to facilitate the development of these applications, it is important to understand the fundamental mechanisms governing terahertz-skin interactions [7,9,18]. To this end, several studies have been conducted to characterize the optical properties of human skin tissues at THz frequencies *ex vivo* [18–21] and *in vivo* [10,22–25]. These studies have successfully used the double Debye model to describe the interaction of THz radiation with human tissues. In this model, the dielectric permittivity function is given by

$$\hat{\epsilon}(\omega) = \epsilon_\infty + \frac{\epsilon_s - \epsilon_2}{1 + i\omega\tau_1} + \frac{\epsilon_2 - \epsilon_\infty}{1 + i\omega\tau_2} \quad (1)$$

where ϵ_∞ is the high frequency limiting value, ϵ_s is the static dielectric constant, ϵ_2 is an intermediate frequency limit, τ_1 and τ_2 are time constants characterizing a slow and a fast relaxation process respectively, and ω is the angular frequency [26,27].

Melanin is the pigment that gives human skin, hair and eyes their color [28–31]. Melanin is synthesized, stored, and transported in pigment-containing organelles known as melanosomes [32,33]. Melanosomes are found within melanocytes, which are the cells

#361269 https://doi.org/10.1364/BOE.10.002942
Journal © 2019 Received 4 Mar 2019; revised 15 May 2019; accepted 15 May 2019; published 22 May 2019

Biomedical Optics EXPRESS

responsible for producing melanin. For the same body region, people possess a similar number of melanocytes in their skin regardless of skin color [28,33]. As melanosomes are filled with melanin, the melanocytes donate them to surrounding skin cells known as keratinocytes. Melanosomes found in the keratinocytes are primarily responsible for the skin's reflectance and they vary in size, shape, number, and amount of melanin they carry depending on the color of the skin [28,33]. In dark skin, melanosomes are larger, more numerous, and more pigmented, *i.e*. containing more melanin, than in intermediate and light skin [28]. Melanosomes and melanin are an integral component of skin [29]. Therefore, in order to develop any medical application of THz light for evaluation or treatment of human skin, it is critical to understand the interaction of THz radiation with skin pigmentation.

Studies on the influence of the concentration and distribution of melanosomes and melanin on the THz spectroscopic properties of skin are extremely sparse [34]. In this study, we used THz time-domain spectroscopy (THz-TDS) to determine the THz optical properties of human skin tissue models comprised of melanocytes from three donor types: Asian, Black, and Caucasian. These skin models exhibit morphological, biochemical, and growth characteristics similar to normal human skin [35], and have been previously assessed as *in vitro* models for studies on pigmentation [36]. Skin models were cultured for three weeks to promote gradual differentiation, the production of melanin, known as melanogenesis, and the transport of melanosomes to the surrounding keratinocytes. We collected THz spectra at various times intervals. The spectra were used to extract the frequency dependent absorption coefficient and index of refraction, *i.e*. optical properties, of the tissue models at THz frequencies. Our results show that there are significant differences in the THz optical properties of the skin tissue models studied both, when comparing their developmental stage and when comparing across the ethnic origin of the donors. These observations highlight the need for further studies into the relationship between the THz optical properties of a tissue and its biomolecular structure.

2. Materials and methods

2.1 Human 3D skin tissue models

In order to examine the influence of melanosomes and melanin on the THz optical properties of skin, we used MelanoDerm viable reconstituted 3-dimensional human skin tissue models from MatTek Corporation. The MelanoDerm system consists of a co-culture of normal, human-derived epidermal keratinocytes (NHEK) and melanocytes that were derived from neonatal foreskins of Asian, Black, or Caucasian donors with a 1/10 ratio of melanocytes to keratinocytes. As the tissues develop over the course of three weeks, they form a multilayer, highly differentiated system with varying amounts of melanin depending on the donor type [36]. According to the manufacturer, after 14 days, the Asian derived tissue contains 20 μg of melanin, the Black derived tissue 48 μg, and the Caucasian derived tissue 10 μg [37].

Each skin tissue model was grown for 2, 8 or 16 days on collagen-coated microporous polytetrafluoroethylene (PTFE) membranes within 9 mm Millipore Millicell CM inserts at the air-liquid interface (ALI) according to the manufacturer's instruction, see Fig. 1(a). Figure 1, panels (b-d), show the pigmentation in all three donor skin tissue models after differentiation.

Biomedical Optics EXPRESS

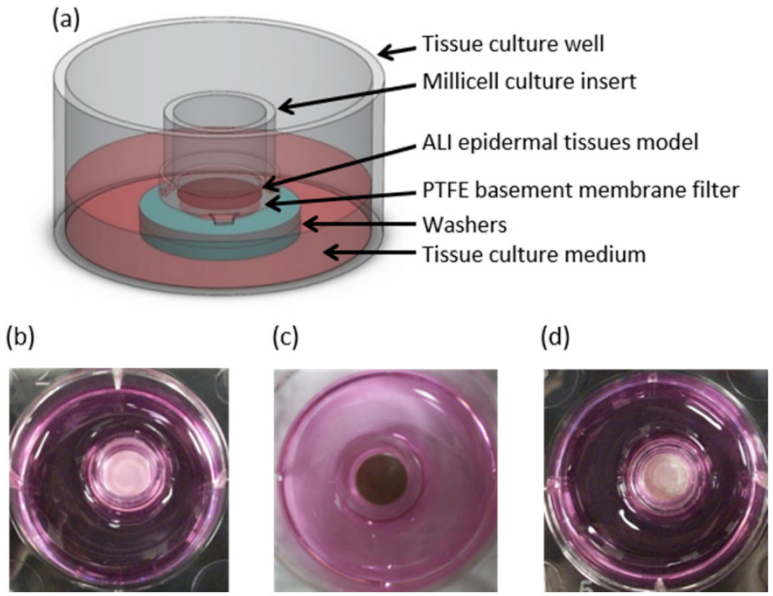

Fig. 1. Human skin tissue model. (a) Schematic illustration of the wells used for culturing skin tissue models. (b-d) Top down digital photographs of (b) Asian, (c) Black, and (d) Caucasian skin tissue models on Day 16.

2.2 THz time-domain measurements

The THz measurements were performed with a Z-3 THz time-domain spectrometer (THz TDS) from Zomega Terahertz Corporation in transmission geometry. A Mai Tai HP Ti:Sapphire laser (Spectraphysics) tuned to 800 nm (<100 fs pulse width, 80 MHz repetition rate) was used to illuminate a photoconductive antenna for THz generation and an electro-optic ZnTe crystal for THz detection.

On the day of the experiment, the inserts containing individual tissue models were quickly removed from the culture media and were immediately placed into a customized sample holder. The customized sample holder consists of a fixed 90° angle clamp for Ø 0.5" optical posts such that the insert fits into one of the openings [34]. A 10 cm focal length TPX lens was used to focus the THz light to a spot size of ~3 mm. The sample holder was placed such that the focal point of the normally incident THz light was located at the surface of the tissue. The transmitted THz light traveled through the tissue and the collagen-coated PTFE membrane within the insert prior to being collected and collimated with a similar lens before going into the detector module. The transmission spectra of the collagen-coated PTFE membrane was measured and found to be relatively flat in the 0.4 to 1.4 THz frequency range, with an average transmissivity of 85% (data not shown). The time taken to mount the samples and perform the measurements was kept consistent among all three samples in order to maintain the tissue hydration levels comparable to each other.

Measurements were collected on the same day for all three donor tissue types; on Day 2 and Day 16. These two time points were chosen to highlight the effects of cell differentiation and melanogenesis. Data were collected at room temperature after purging the chamber with dry air for 5 minutes in order to eliminate any atmospheric water. The sample chamber filled with dry air sans sample was used as a reference. The spectrometer measures signals that are proportional to the transmitted THz electric field as a function of time, *i.e.* time domain waveforms. We used one sample per tissue type and took two time domain measurements for each sample, including the reference. The time domain data of the two measurements were nominally the same, indicating that there were no measurable changes in the water content of

Biomedical Optics EXPRESS

the tissues during the time it took to obtain the data. Therefore, the two time domain measurements were averaged before obtaining the THz spectra by performing a Fourier transform using a custom-written Matlab (Mathworks) program.

2.3 Tissue thickness measurements

The skin tissue equivalents differentiate over the course of three weeks. During this time their overall thickness increases. In order to determine the tissues thicknesses, the culture of the epidermal tissues was stopped at Day 2, 8, and 16 to perform histological sections. For histology, the epidermal tissues were removed from the inserts and were fixed at room temperature in 10% neutral buffered formalin. For each tissue, formalin fixation was done on the exact same sample following THz measurements. The fixed tissues were embedded in paraffin, sectioned, and stained. The sections were used to measure the thickness of the stratum corneum, epidermis, and dermis with an optical microscope (data not shown). The fixation and sectioning process caused some delamination of the tissue layers, so each layer was measured individually. These measurements were added together to determine the total thickness. Multiple measurements (≥4) were performed on several slides and at different locations per slide for each tissue type (column labeled # in Table 1).

2.4 THz optical parameter extraction

The Fourier transform of the time domain waveforms allows us to obtain the complex, *i.e.* amplitude and phase, THz spectra in the frequency domain. The complex transmission spectrum of each skin tissue model was obtained by taking the ratio $E_s(\omega)/E_r(\omega)$ where $E_s(\omega)$ and $E_r(\omega)$ are the spectra of the sample and the reference respectively, and ω is the angular frequency. The complex transmission spectra was used to extract the frequency dependent absorption coefficient $\alpha(\omega)$ and index of refraction $n(\omega)$ as

$$\alpha(\omega) = \frac{1}{d}\log\left(\left[\frac{|E_s|}{|E_r|}\right]^2\right) \tag{2}$$

and

$$n(\omega) = 1 + \frac{c(\varphi_s - \varphi_r)}{\omega d} \tag{3}$$

where d is the sample thickness, c is the speed of light in vacuum, and φ_s and φ_r are the phase spectra of the sample and the reference, respectively [38]. Although the THz spectrometer used can measure from 0.1 to 3 THz, we have only presented the data between 0.4 and 1.4 THz because of the high absorption observed above 1.4 THz and the poor signal to noise outside that frequency range. Note that we do not observe multiple reflections and, consequently, have neglected any Fabry-Perot effects.

3. Results

3.1 Thickness measurements

Table 1 reports the measurements on the thickness obtained from the optical images for the fixed skin tissue models on Days 2, 8, and 16. In the analysis to extract the THz optical parameters, we used this thickness value given that we are performing transmission measurements and were unable to resolve different layers in the time domain data.

Biomedical Optics EXPRESS

Table 1. Skin tissue model thickness[a]

	Asian	#	Black	#	Caucasian	#
Day 2	122.8 ± 4.0	7	118.2 ± 11.0	7	107.0 ± 7.1	4
Day 8	184.9 ± 7.2	4	206.6 ± 17.1	4	194.5 ± 12.2	4
Day 16	237.9 ± 19.7	4	260.3 ± 9.9	5	262.6 ± 10.6	5

[a]All measurements are reported in microns as (mean ± SD) and # is the number of measurements on each tissue.

3.2 Absorption coefficient and index of refraction of skin tissue models

Figures 2(a) and 2(b) show the absorption coefficient and index of refraction for the three skin tissue models on Day 2 and Day 16. In all cases the data show that the absorption coefficient is between 70 and 300 cm^{-1} and increases with frequency. The index of refraction is between 1.4 and 2.7 and decreases with frequency. We determined that the differences in the absorption coefficient and index of refraction between all three tissue types were statistically significant by performing a two-sample *t*-test. The error bars were obtained from the absorption coefficient and index of refraction calculated by adding and subtracting the standard deviation (SD) from the mean thicknesses from Table 1. Note that the uncertainty in determining the absorption coefficient and index of refraction is dominated by the error in specifying the tissue thickness, not the variability in the THz time domain measurements.

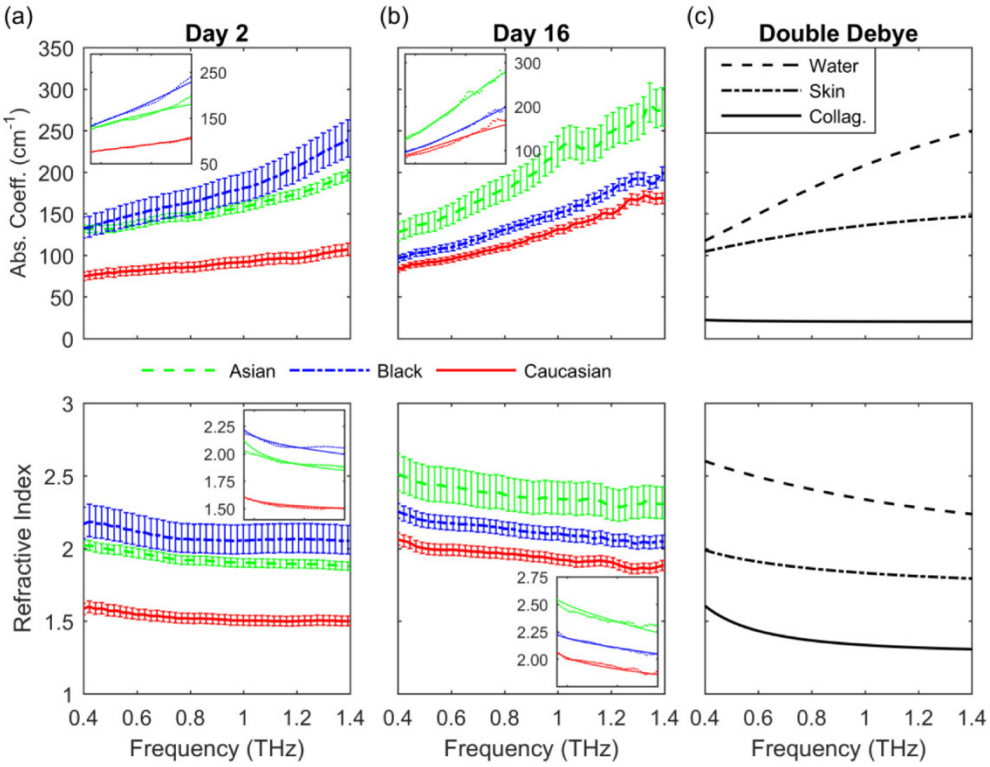

Fig. 2. THz optical properties of (a) Asian, Black, and Caucasian donor tissue models on Day 2, (b) on Day 16, and of (c) water, skin, and collagen obtained from the double Debye model. Insets: fits from the double Debye model.

Figure 2(c) shows the results of using the double Debye model to obtain the absorption coefficient and index of refraction of water, skin, and collagen by using parameters found in the literature [26,39]. The values obtained in our study are consistent with the values obtained

Biomedical Optics EXPRESS

from the double Debye model, with other measurements of human epithelial tissue [7,22] and our own experiments which examined the optical properties of human skin *in vivo* at THz frequency using a compact THz TDS system in a reflection geometry [23]. The trend of the absorption coefficient and the index of refraction of the skin tissue models follow that of water as expected [7].

Figure 2(a) shows that, in general, the absorption coefficient and index of refraction of the Asian donor tissue model on Day 2 are comparable to those of the Black donor tissue type over the entire frequency range. However, at frequencies above 1 THz, the absorption coefficient and index of refraction of the Black donor tissue model are both slightly larger than those of the Asian donor tissue type. The absorption coefficient and index of refraction of the Caucasian donor tissue model, on the other hand, are both significantly smaller than those of the Asian and Black donor tissue types.

On Day 16, Fig. 2(b), the difference between the absorption coefficient and index of refraction of the Asian and Black donor tissue models increases relative to those of Day 2. The largest difference between the absorption coefficient of the Asian and Black donor tissue models remains at frequencies above 1 THz. The absorption coefficient and index of refraction are both consistently larger for the Asian donor tissue model compared to those for the Black or Caucasian donor tissue types, with the Caucasian type always being the smallest. The large differences between the absorption coefficient and index of refraction of the Black and Caucasian donor tissue models observed on Day 2 are not present on Day 16.

The absorption coefficient and index of refraction of the Asian and Caucasian donor tissue models increase as the cells differentiate as shown in Figs. 2(a) and 2(b). However, the absorption coefficient of the Black donor tissue model decreased from Day 2 to Day 16, while the index of refraction remained approximately the same, increasing only, on average, by 2%. The absorption coefficient and index of refraction of the Caucasian donor tissue model are always the smallest as compared to those of the Asian or Black tissue types, with the largest difference occurring in Day 2.

3.3 Extraction of double Debye parameters

It is widely accepted that the THz permittivity of biological tissues is described by a double Debye model. To validate our results we simultaneously fitted the absorption coefficient and index of refraction to a double Debye model using a nonlinear least-squares fit (see insets in Figs. 1 (a)-(b) and Appendix 1 for details). Table 2 reports the dielectric relaxation parameters (ϵ_s, ϵ_2, ϵ_∞, τ_1, and τ_2) obtained for each skin tissue type for Day 2 and Day 16.

Table 2. Dielectric relaxation parameters from double Debye model

		ϵ_s	ϵ_2	ϵ_∞	τ_1 (ps)	τ_2 (ps)
Day 2	**Asian**	23	3.5	3.0	2.5	0.10
	Black	78	4.2	2.8	9.0	0.07
	Caucasian	27	2.3	2.0	7.0	0.07
Day 16	**Asian**	88	6.0	3.5	10.5	0.11
	Black	66	4.6	3.0	11.0	0.08
	Caucasian	21	3.8	2.9	3.5	0.11

The dielectric relaxation parameters obtained for the Asian and the Caucasian donor tissue types on Day 2 are, in general, lower than those obtained for Day 16, reflecting the changes in the tissues as they differentiate. The parameters obtained for the Black donor tissue model on Day 2 and Day 16 are comparable to each other, reflecting the small changes observed in the

Biomedical Optics EXPRESS

THz measurements. The parameters obtained for all three tissue types on both days are comparable to those previously reported in the literature for human skin tissue [27,40].

3.4 Normalized percentage difference between donor types

In order to highlight and quantify the differences between the THz optical properties of the three donor tissue types, we calculated the normalized percentage difference between Asian and Black donor tissue models relative to the Caucasian donor tissue type and between the Asian and Black donor tissue model for Days 2 and 16. The normalized percentage difference between Asian and Black donor tissue models relative to the Caucasian donor tissue type was calculated as $\%Diff.=100\times\left|\frac{X_i-X_C}{X_C}\right|$, where X is either α or n, the subscript i represents the Asian or the Black donor tissue model, the subscript C refers to the Caucasian donor tissue model, and $|\,|$ represents the absolute value. Similarly, for the normalized percentage difference between the Asian and Black donor tissue model we calculated $\%Diff.=100\times\left|\frac{X_A-X_B}{X_B}\right|$, where the subscripts A and B represent the Asian and the Black donor tissue model respectively.

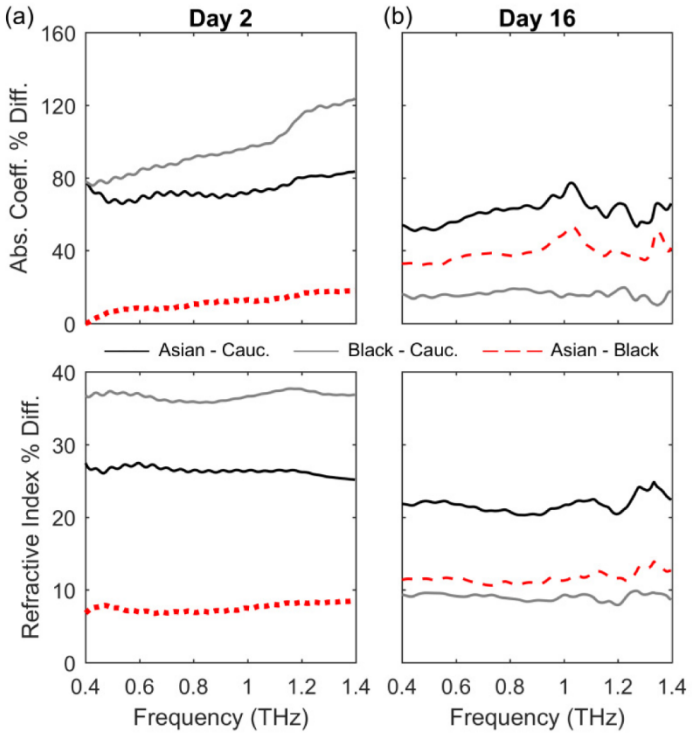

Fig. 3. Normalized percentage difference of the absorption coefficient (top) and index of refraction (bottom) for (a) Day 2 and (b) Day 16.

In Fig. 3 it can be observed that the largest differences occur on Day 2, with differences of up to 120% for the absorption coefficient at 1.4 THz and an average of (36.7 ± 0.6) % for the index of refraction of the Black donor tissue type relative to that of the Caucasian donor, gray solid lines in Fig. 3(a). All averages are reported as (mean ± SD). Note that the normalized percentage difference in the index of refraction of all three tissue types is relatively flat across the entire frequency range. The difference between the Asian and Caucasian donor tissue

Biomedical Optics EXPRESS

models' absorption coefficient has an average value of (73.4 ± 4.9) % while the normalized percentage difference in the index of refraction is (26.4 ± 0.5) %, black lines in Fig. 3(a). The normalized percentage difference in the absorption coefficient of the Asian donor tissue model relative to the Black donor tissue type remains below 12% throughout the entire frequency range, with the largest difference occurring at 1.4 THz (dotted red line). On average, the normalized percentage difference in the index of refraction of the Asian donor tissue model relative to the Black donor tissue type is (7.5 ± 0.5) %, dotted red line in Fig. 3(a) bottom panel. Note that the absorption coefficient and the index of refraction of the Asian donor tissue model are smaller than those of the Black donor tissue type on Day 2, Fig. 2(a), therefore the normalized percentage differences for the absorption coefficient and the index of refraction in Fig. 3(a) are negative.

On Day 16, the largest normalized percentage differences occur between the Asian and Caucasian donor tissue types with differences, on average, of (61.2 ± 6.3) % for the absorption coefficient and (21.7 ± 1.0) % for the index of refraction, black lines in Fig. 3(b). In Fig. 3(b), it can be seen that the differences between the absorption coefficient and index of refraction of the Asian and Black donor tissue types have average values of (39.1 ± 5.2) % and (11.6 ± 0.7) % respectively (dashed red lines), while those between the Black and Caucasian donor tissue types are (15.9 ± 1.9) % for the absorption coefficient and (9.1 ± 0.4) % for the index of refraction (gray lines).

4. Discussion

In this study we have measured the THz optical properties of three different skin donor tissue models as the tissues differentiate and become more pigmented. We have shown that there are significant differences in their optical properties when comparing across different donor phenotypes (Asian, Black or Caucasian) and when comparing their developmental stage (Day 2 vs. Day 16). In order to confirm the validity of these observations, we extracted the dielectric relaxation parameters from double Debye fits and found that they are comparable to those previously reported for human skin. We compared the normalized percentage difference in the absorption coefficient and in the index of refraction observed between the three skin donor tissue models in Day 16 (>16% for the absorption coefficient and >9% for the index of refraction) to those previously observed between human basal cell carcinoma and healthy tissues (<20% for the absorption coefficient and <2.6% for the index of refraction) [7]. In addition, we calculated the real and imaginary parts of the dielectric permittivity for each donor tissue type (see Appendix 2, Fig. 4) and compared them to those for healthy tissue, dysplastic and non-dysplastic skin nevi found in the literature [10,27,41]. In all cases our data compared favorably to those studies, further supporting our results.

From comparing the THz optical properties between different skin donor models, it is clear that there are significant differences in their optical properties in Day 2. These differences are accentuated as the tissue differentiates and are more apparent on Day 16, when the tissues more closely represent a fully developed epidermal tissue. Based on the development process of skin tissue, Day 2 samples would exhibit very few melanosomes and, correspondingly, very little melanin content. Therefore, we can infer that the differences in the THz optical properties of the three tissue models at this time point are not a direct result of the level of melanin present. By Day 16, the cells have differentiated, melanin has been produced and transported within melanosomes to the keratinocytes. As expected, the Black donor tissue model contains more melanin than either the Asian or the Caucasian donor tissue models [37]. Surprisingly, the absorption coefficient and the index of refraction of the Black donor tissue model are both smaller than those of the Asian donor tissue model. Therefore, the measurements obtained on Day 16 support the conclusion that the melanin content is not solely responsible for the differences in the THz optical properties of the three tissue models.

The absorption coefficient and index of refraction of the Asian and Caucasian donor tissue types increased from Day 2 to Day 16. In contrast, the absorption coefficient of the Black

Biomedical Optics EXPRESS

donor tissue model decreased while the index of refraction increased very slightly. It is known that dark skin contains more melanosomes than lighter skin, with the melanosomes being larger and containing more melanin. We speculate that having a bigger number of larger and darker melanosomes increases the scattering within the tissue, affecting the THz transmission [42] and producing the counterintuitive results observed for the Black donor tissue model.

There are other factors that influence the biomolecular structure of skins of different ethnicities in addition to the size and number of melanosomes. Some of these factor are cell density [43], amount and type of collagen [44], lipid content [45,46], protein concentration [29,31], as well as type of melanin, melanosome shape and distribution [47,48]. All of these factors may potentially affect the THz optical properties of skin to varying degrees and could be responsible for the differences in the relaxation parameters obtained from the double Debye fits [7]. Moreover, some of these factors change with age in different manners depending on ethnicity and from one body part to another [31,46,49], further supporting the need for studies to elucidate their contribution to the THz response of human skin for the effective development of medical applications of THz light.

The skin donor tissue models used in this manuscript are from Asian, Black, and Caucasian donors. A visual reference for the appearance of these different tissue models is shown in Figs. 1 (b)-(d). However, these images do not provide an objective measure of the degree of pigmentation of the tissue models measured. One way to objectively characterize the color of the skin used in the dermatological community is to measure the luminosity L* of a tissue, where the luminosity is the perceived brightness of an object by a human observer. L* is also referred to as the lightness value in the CIELAB color space, where L* = 0 yields black and L* = 100 indicates diffuse white [50,51]. In order to eliminate any artifacts due to illumination conditions, measurements of the luminosity are performed by quantifying the intensity of light reflected from the tissue using a spectrophotometer under daylight (D65) standard illumination. The L* value has been found to be correlated to the product of the melanocyte to epidermal cell ratio and the melanocytes' melanin content [52]. The luminosity of skins has been reported in [49] for African American as L*~43 and Caucasians as L*~63. Our results suggest that future investigations into the THz spectroscopy of human skin should include measurements of the luminosity or some other objective measurement of the skin color in order to be able to compare across different studies effectively. Given recent developments on the relationship between genetics and the diversity in human skin pigmentation [53,54], moving away from ethnic descriptors is also advised.

The measurements performed in our study were done in transmission geometry. However, our results can be transferred to measurements of tissue in reflection geometry. In particular, when conducting THz studies on skin hydration for evaluating edema [55,56], researchers should consider the differences observed in the values of the absorption coefficient of the Asian donor skin tissue model versus that of the Caucasian donor given that the absorption coefficient of the former is closer to that of water under the same conditions, resulting in pulse broadening. In addition, when conducting THz imaging studies of skin, researchers need to take into consideration that having a larger index of refraction, such as that observed in the Asian donor tissue model as compared to the Caucasian donor tissue model, will result in a stronger reflected signal and can impact the interpretation of their observations.

5. Conclusion

In summary, we used THz time domain spectroscopy to measure the THz optical properties of *in vitro* pigmented human skin tissue models during melanogenesis. The absorption coefficient and index of refraction obtained for all skin tissue models fall within the acceptable range for pure collagen and water, and are comparable to those obtained in other studies on human skin. For all skin tissue models studied, the results show that as the frequency increases, the absorption coefficient increases while the index of refraction

Biomedical Optics EXPRESS

decreases, and there are no salient features. Our results support the notion that factors other than melanin content may be contributing to the THz optical properties of the three different skin tissue models studied. These factors are probably related to the differences in the biomolecular structure of human skin of different ethnic origin. These observations highlight the need for a better understanding of how THz radiation interacts with the biomolecular structure of tissues. An increased understanding of the fundamental mechanisms governing THz-human skin interactions is critical for the development of any type of effective medical application of THz light.

Appendix 1. Fits to double Debye model

We wrote a program in Matlab to find the combination of dielectric relaxation parameters (ϵ_s, ϵ_2, ϵ_∞, τ_1, and τ_2) that best fit both the absorption coefficient and the index of refraction obtained from the THz complex transmission spectra. In the double Debye model, the dielectric permittivity function is given by Eq. (4)

$$\hat{\epsilon}(\omega) = \epsilon_\infty + \frac{\epsilon_s - \epsilon_2}{1 + i\omega\tau_1} + \frac{\epsilon_2 - \epsilon_\infty}{1 + i\omega\tau_2} \tag{4}$$

where ϵ_∞ is the high frequency limiting value, ϵ_s is the static dielectric constant, ϵ_2 is an intermediate frequency limit, τ_1 and τ_2 are time constants characterizing a slow and a fast relaxation process respectively, and ω is the angular frequency. In addition, we know that the complex dielectric permittivity is related to the absorption coefficient and the index of refraction by $\hat{\epsilon}(\omega) = \epsilon'(\omega) - i\epsilon''(\omega) = \left[n(\omega) - i\frac{c}{2\omega}\alpha(\omega) \right]^2$. From this relationship we can define the fitting functions as

$$\alpha_{fit}(\omega) = \frac{2\omega}{c}\left(\frac{\sqrt{Re(\hat{\epsilon})^2 + Im(\hat{\epsilon})^2} - Re(\hat{\epsilon})}{2} \right)^{1/2} \tag{5}$$

and

$$n_{fit}(\omega) = \left(\frac{\sqrt{Re(\hat{\epsilon})^2 + Im(\hat{\epsilon})^2} + Re(\hat{\epsilon})}{2} \right)^{1/2} \tag{6}$$

where $Re(\hat{\epsilon})$ is the real part and $Im(\hat{\epsilon})$ is the imaginary part of Eq. (4). The best fit was chosen as to minimize the sum of squares of the residuals given by

$$SSR = \sum_{i=1}^{m} \left[\left(\alpha_i - \alpha_{fit,i} \right)^2 + \left(n_i - n_{fit,i} \right)^2 \right] \tag{7}$$

where α_i (n_i) is the i-th absorption coefficient (index of refraction) data point obtained from the complex transmission spectra, $\alpha_{fit,i}$ and $n_{fit,i}$ are the corresponding data points obtained from the fit, and m is the number of data points in the data set. Figure 4 shows the results of the best fits which result in the parameters presented in Table 2 together with the corresponding measurements of the absorption coefficient and index of refraction.

Biomedical Optics EXPRESS

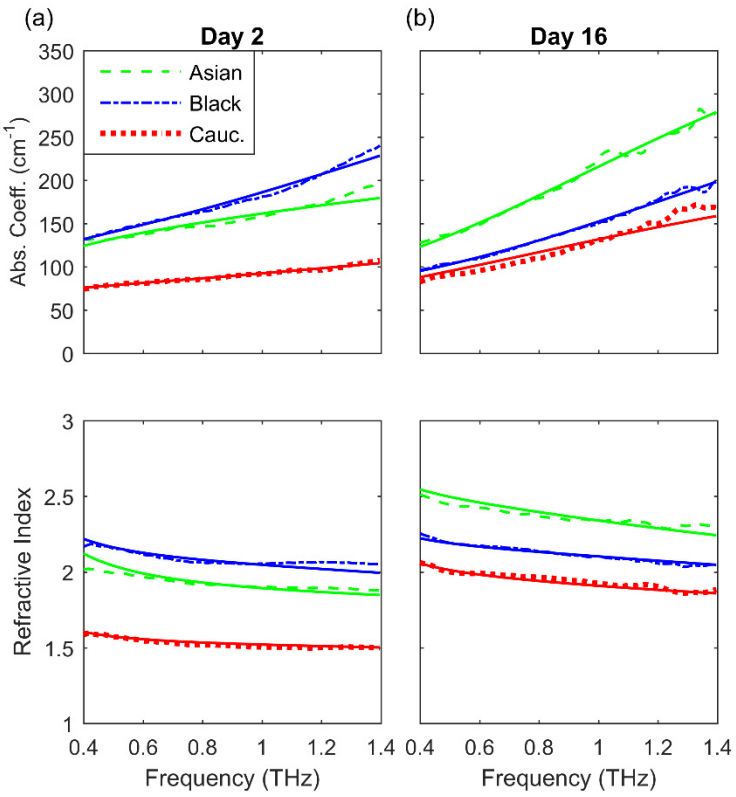

Fig. 4. Absorption coefficient (top) and index of refraction (bottom) obtained from the complex transmission spectra (dashed lines) and the double Debye model (solid lines) for (a) Day 2 and (b) Day 16.

Appendix 2. Calculations of dielectric permittivity function

We used the absorption coefficient and the index of refraction obtained from the THz complex transmission spectra to calculate the real and imaginary parts of the complex dielectric permittivity as $\hat{\epsilon}(\omega) = \epsilon'(\omega) - i\epsilon''(\omega)$ where the real part is given by $\epsilon'(\omega) = n(\omega)^2 - \left(\frac{c}{2\omega}\right)^2 \alpha(\omega)^2$ and the imaginary part by $\epsilon''(\omega) = \left(\frac{c}{\omega}\right)\alpha(\omega)n(\omega)$. Figures 5(a) and 5(b) show plots of the real and imaginary parts of the dielectric permittivity as a function of frequency for the three donor tissue types on Day 16 while Fig. 5(c) is a Cole-Cole diagram. From Fig. 5 it can be seen that, both, the real and imaginary parts of the dielectric permittivity decrease monotonically as a function of frequency and have no salient features between 0.4 and 1.4 THz. The real part of the dielectric permittivity ranges from 3.2 to 5.8 while the imaginary part is found between 1 and 4. The range of values reported for the real part of the dielectric permittivity of normal, healthy tissues in reference [10] are 2.5 to 3.5 between 0.3 and 1 THz, while those reported in reference [41] are 3.6 to 5.8 between 0.3 and 3 THz. The range of values reported for the imaginary part of the dielectric permittivity of normal, healthy tissues in reference [10] are 1 to 3.5 between 0.3 and 1 THz, and 2 to 4.1 between 0.3 and 3 THz in reference [41]. Our data compares favorably to those studies.

Biomedical Optics EXPRESS

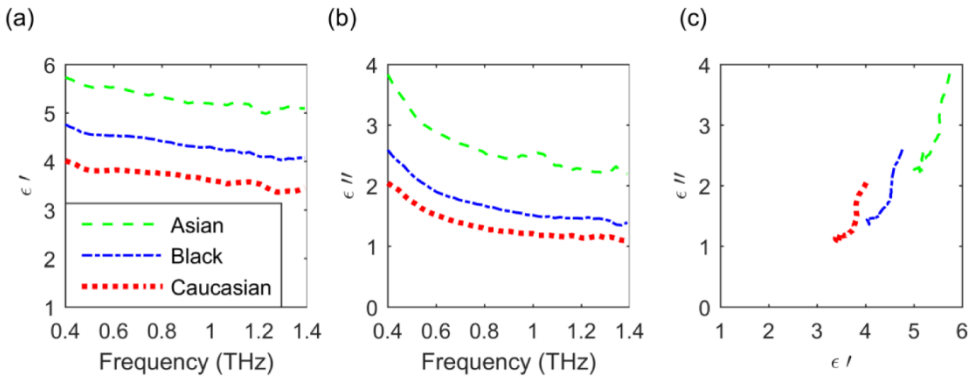

Fig. 5. Complex dielectric permittivity of the three tissue models. (a) Real and (b) imaginary parts. (c) Cole-Cole diagram.

Funding

Air Force Research Laboratory, Airman Systems Directorate; National Science Foundation Partnerships for Research and Education in Materials (NSF-PREM) (DMR-0934218). This research was performed while X.G.P. (currently) and I.E. (formerly) held NRC Research Associateship awards at the Air Force Research Laboratory.

Disclosures

The authors declare that there are no conflicts of interest related to this article.

References

1. Z. D. Taylor, R. S. Singh, M. O. Culjat, J. Y. Suen, W. S. Grundfest, H. Lee, and E. R. Brown, "Reflective terahertz imaging of porcine skin burns," Opt. Lett. **33**(11), 1258–1260 (2008).
2. M. Dutta, A. S. Bhalla, and R. Guo, "THz Imaging of Skin Burn: Seeing the Unseen-An Overview," Adv. Wound Care (New Rochelle) **5**(8), 338–348 (2016).
3. M. H. Arbab, T. C. Dickey, D. P. Winebrenner, A. Chen, M. B. Klein, and P. D. Mourad, "Terahertz reflectometry of burn wounds in a rat model," Biomed. Opt. Express **2**(8), 2339–2347 (2011).
4. Z. D. Taylor, R. S. Singh, D. B. Bennett, P. Tewari, C. P. Kealey, N. Bajwa, M. O. Culjat, A. Stojadinovic, H. Lee, J.-P. Hubschman, E. R. Brown, and W. S. Grundfest, "THz Medical Imaging: in vivo Hydration Sensing," IEEE Trans. Terahertz Sci. Technol. **1**(1), 201–219 (2011).
5. P. Tewari, C. P. Kealey, D. B. Bennett, N. Bajwa, K. S. Barnett, R. S. Singh, M. O. Culjat, A. Stojadinovic, W. S. Grundfest, and Z. D. Taylor, "In vivo terahertz imaging of rat skin burns," J. Biomed. Opt. **17**(4), 040503 (2012).
6. N. Bajwa, "In vivo terahertz imaging of tissue edema for burn wound and flap assessment - eScholarship," UCLA (2016).
7. V. P. Wallace, A. J. Fitzgerald, E. Pickwell, R. J. Pye, P. F. Taday, N. Flanagan, and T. Ha, "Terahertz Pulsed Spectroscopy of Human Basal Cell Carcinoma," Appl. Spectrosc. **60**(10), 1127–1133 (2006).
8. R. M. Woodward, V. P. Wallace, D. D. Arnone, E. H. Linfield, and M. Pepper, "Terahertz Pulsed Imaging of Skin Cancer in the Time and Frequency Domain," J. Biol. Phys. **29**(2), 257–259 (2003).
9. C. Yu, S. Fan, Y. Sun, and E. Pickwell-Macpherson, "The potential of terahertz imaging for cancer diagnosis: A review of investigations to date," Quant. Imaging Med. Surg. **2**(1), 33–45 (2012).
10. K. I. Zaytsev, N. V. Chernomyrdin, K. G. Kudrin, A. A. Gavdush, P. A. Nosov, S. O. Yurchenko, and I. V. Reshetov, "In vivo terahertz pulsed spectroscopy of dysplastic and non-dysplastic skin nevi," J. Phys. Conf. Ser. **735**, 012076 (2016).
11. K. Shiraga, Y. Ogawa, T. Suzuki, N. Kondo, A. Irisawa, and M. Imamura, "Characterization of Dielectric Responses of Human Cancer Cells in the Terahertz Region," J. Infrared Millim. Terahertz Waves **35**(5), 493–502 (2014).
12. K. W. Kim, K.-S. Kim, H. Kim, S. H. Lee, J.-H. Park, J.-H. Han, S.-H. Seok, J. Park, Y. Choi, Y. I. Kim, J. K. Han, and J.-H. Son, "Terahertz dynamic imaging of skin drug absorption," Opt. Express **20**(9), 9476–9484 (2012).
13. K.-T. Kim, J. Park, S. J. Jo, S. Jung, O. S. Kwon, G. P. Gallerano, W.-Y. Park, and G.-S. Park, "High-power femtosecond-terahertz pulse induces a wound response in mouse skin," Sci. Rep. **3**(1), 2296 (2013).

Biomedical Optics EXPRESS

14. L. V. Titova, A. K. Ayesheshim, A. Golubov, R. Rodriguez-Juarez, R. Woycicki, F. A. Hegmann, and O. Kovalchuk, "Intense THz pulses down-regulate genes associated with skin cancer and psoriasis: a new therapeutic avenue?" Sci. Rep. **3**(1), 2363 (2013).
15. R. Williams, A. Schofield, G. Holder, J. Downes, D. Edgar, P. Harrison, M. Siggel-King, M. Surman, D. Dunning, S. Hill, D. Holder, F. Jackson, J. Jones, J. McKenzie, Y. Saveliev, N. Thomsen, P. Williams, and P. Weightman, "The influence of high intensity terahertz radiation on mammalian cell adhesion, proliferation and differentiation," Phys. Med. Biol. **58**(2), 373–391 (2013).
16. I. Echchgadda, C. Z. Cerna, M. A. Sloan, D. P. Elam, and B. L. Ibey, "Effects of different terahertz frequencies on gene expression in human keratinocytes," in *Proc.SPIE* (2015), Vol. 9321.
17. G. J. Wilmink and J. E. Grundt, "Invited Review Article: Current State of Research on Biological Effects of Terahertz Radiation," J. Infrared Millim. Terahertz Waves **32**(10), 1074–1122 (2011).
18. A. J. Fitzgerald, E. Berry, N. N. Zinov'ev, S. Homer-Vanniasinkam, R. E. Miles, J. M. Chamberlain, and M. A. Smith, "Catalogue of human tissue optical properties at terahertz frequencies," J. Biol. Phys. **29**(2), 123–128 (2003).
19. G. M. Png, J. W. Choi, B. W.-H. Ng, S. P. Mickan, D. Abbott, and X.-C. Zhang, "The impact of hydration changes in fresh bio-tissue on THz spectroscopic measurements," Phys. Med. Biol. **53**(13), 3501–3517 (2008).
20. S. Y. Huang, Y. X. J. Wang, D. K. W. Yeung, A. T. Ahuja, Y.-T. Zhang, and E. Pickwell-Macpherson, "Tissue characterization using terahertz pulsed imaging in reflection geometry," Phys. Med. Biol. **54**(1), 149–160 (2009).
21. Y. Sun, M. Y. Sy, Y.-X. J. Wang, A. T. Ahuja, Y.-T. Zhang, and E. Pickwell-Macpherson, "A promising diagnostic method: Terahertz pulsed imaging and spectroscopy," World J. Radiol. **3**(3), 55–65 (2011).
22. E. Pickwell, B. E. Cole, A. J. Fitzgerald, M. Pepper, and V. P. Wallace, "In vivo study of human skin using pulsed terahertz radiation," Phys. Med. Biol. **49**(9), 1595–1607 (2004).
23. I. Echchgadda, J. A. Grundt, M. Tarango, B. L. Ibey, T. Tongue, M. Liang, H. Xin, and G. J. Wilmink, "Using a portable terahertz spectrometer to measure the optical properties of in vivo human skin," J. Biomed. Opt. **18**(12), 120503 (2013).
24. S. Fan, B. S. Y. Ung, E. P. J. Parrott, V. P. Wallace, and E. Pickwell-MacPherson, "In vivo terahertz reflection imaging of human scars during and after the healing process," J. Biophotonics **10**(9), 1143–1151 (2017).
25. Q. Sun, E. P. J. Parrott, Y. He, and E. Pickwell-MacPherson, "In vivo THz imaging of human skin: Accounting for occlusion effects," J. Biophotonics **11**(2), e201700111 (2018).
26. E. Pickwell, B. E. Cole, A. J. Fitzgerald, V. P. Wallace, and M. Pepper, "Simulation of terahertz pulse propagation in biological systems," Appl. Phys. Lett. **84**(12), 2190–2192 (2004).
27. B. C. Truong, H. D. Tuan, H. H. Kha, and H. T. Nguyen, "Debye parameter extraction for characterizing interaction of terahertz radiation with human skin tissue," IEEE Trans. Biomed. Eng. **60**(6), 1528–1537 (2013).
28. G. S. Barsh, "What Controls Variation in Human Skin Color?" PLoS Biol. **1**(1), E27 (2003).
29. V. J. Hearing, "Biogenesis of pigment granules: a sensitive way to regulate melanocyte function," J. Dermatol. Sci. **37**(1), 3–14 (2005).
30. P. A. Riley, "Melanin," Int. J. Biochem. Cell Biol. **29**(11), 1235–1239 (1997).
31. F. Solano, "Melanins: Skin Pigments and Much More—Types, Structural Models, Biological Functions, and Formation Routes," https://www.hindawi.com/archive/2014/498276/.
32. Y. Yamaguchi and V. J. Hearing, "Physiological factors that regulate skin pigmentation," Biofactors **35**(2), 193–199 (2009).
33. M. S. Marks and M. C. Seabra, "The melanosome: Membrane dynamics in black and white," Nat. Rev. Mol. Cell Biol. **2**(10), 738–748 (2001).
34. D. Lipscomb, I. Echchgadda, X. G. Peralta, and G. J. Wilmink, "Determination of the optical properties of melanin-pigmented human skin equivalents using terahertz time-domain spectroscopy," in G. J. Wilmink and B. L. Ibey, eds. (2013), p. 85850F.
35. N. A. Monteiro-Riviere, A. O. Inman, T. H. Snider, J. A. Blank, and D. W. Hobson, "Comparison of an in vitro skin model to normal human skin for dermatological research," Microsc. Res. Tech. **37**(3), 172–179 (1997).
36. T.-J. Yoon, T. C. Lei, Y. Yamaguchi, J. Batzer, R. Wolber, and V. J. Hearing, "Reconstituted 3-dimensional human skin of various ethnic origins as an in vitro model for studies of pigmentation," Anal. Biochem. **318**(2), 260–269 (2003).
37. M. Bachelor, B. Breyfogle, A. Armento, and M. Klausner, "607 Measurement of Skin Pigmentation Using a Chromameter in a 3-Dimensional Epidermal Model Containing Functional Melanocytes," J. Invest. Dermatol. **136**(5), S108 (2016).
38. J. T. Kindt and C. A. Schmuttenmaer, "Far-Infrared Dielectric Properties of Polar Liquids Probed by Femtosecond Terahertz Pulse Spectroscopy," J. Phys. Chem. **100**(24), 10373–10379 (1996).
39. K. Yang, N. Chopra, Q. Abbasi, K. Qaraqe, and A. Alomainy, "Collagen Analysis at Terahertz Band using Double-Debye Parameter Extraction and Particle Swarm Optimisation," IEEE Access **PP**, 1–1 (2017).
40. E. Pickwell, A. J. Fitzgerald, B. E. Cole, P. F. Taday, R. J. Pye, T. Ha, M. Pepper, and V. P. Wallace, "Simulating the response of terahertz radiation to basal cell carcinoma using ex vivo spectroscopy measurements," J. Biomed. Opt. **10**(6), 064021 (2005).
41. K. Shiraga, Y. Ogawa, T. Suzuki, N. Kondo, A. Irisawa, and M. Imamura, "Determination of the complex dielectric constant of an epithelial cell monolayer in the terahertz region," Appl. Phys. Lett. **102**(5), 053702 (2013).

Biomedical Optics EXPRESS

42. J. Pearce, Z. Jian, D. M. Mittleman, P. Jeremy, Z. Jian, and D. M. Mittleman, "Propagation of terahertz pulses in random media," Philos Trans A Math Phys Eng Sci **362**(1815), 301–313, discussion 313–314 (2004).
43. A. V. Rawlings, "Ethnic skin types: are there differences in skin structure and function?" Int. J. Cosmet. Sci. **28**(2), 79–93 (2006).
44. E. Berardesca, J. de Rigal, J. L. Leveque, and H. I. Maibach, "In vivo biophysical characterization of skin physiological differences in races," Dermatologica **182**(2), 89–93 (1991).
45. W. Montagna and K. Carlisle, "The architecture of black and white facial skin," J. Am. Acad. Dermatol. **24**(6), 929–937 (1991).
46. N. A. Vashi, M. B. de Castro Maymone, and R. V. Kundu, "Aging Differences in Ethnic Skin," J. Clin. Aesthet. Dermatol. **9**(1), 31–38 (2016).
47. "Characterization of Melanogenesis in Normal Human Epidermal Melanocytes by Chemical and Ultrastructural Analysis - NAKAGAWA - 1996 - Pigment Cell & Melanoma Research - Wiley Online Library," http://onlinelibrary.wiley.com/doi/10.1111/j.1600-0749.1996.tb00106.x/abstract.
48. A. Hennessy, C. Oh, B. Diffey, K. Wakamatsu, S. Ito, and J. Rees, "Eumelanin and pheomelanin concentrations in human epidermis before and after UVB irradiation," Pigment Cell Res. **18**(3), 220–223 (2005).
49. A. L. Chien, J. Suh, S. S. A. Cesar, A. H. Fischer, N. Cheng, F. Poon, B. Rainer, S. Leung, J. Martin, G. A. Okoye, and S. Kang, "Pigmentation in African American skin decreases with skin aging," J. Am. Acad. Dermatol. **75**(4), 782–787 (2016).
50. M. D. Shriver and E. J. Parra, "Comparison of narrow-band reflectance spectroscopy and tristimulus colorimetry for measurements of skin and hair color in persons of different biological ancestry," Am. J. Phys. Anthropol. **112**(1), 17–27 (2000).
51. I. L. Weatherall and B. D. Coombs, "Skin color measurements in terms of CIELAB color space values," J. Invest. Dermatol. **99**(4), 468–473 (1992).
52. W.-S. Huang, Y.-W. Wang, K.-C. Hung, P.-S. Hsieh, K.-Y. Fu, L.-G. Dai, N.-H. Liou, K.-H. Ma, J.-C. Liu, and N.-T. Dai, "High correlation between skin color based on CIELAB color space, epidermal melanocyte ratio, and melanocyte melanin content," PeerJ **6**, e4815 (2018).
53. J.-C. Chacón-Duque, K. Adhikari, M. Fuentes-Guajardo, J. Mendoza-Revilla, V. Acuña-Alonzo, R. Barquera, M. Quinto-Sánchez, J. Gómez-Valdés, P. Everardo Martínez, H. Villamil-Ramírez, T. Hünemeier, V. Ramallo, C. C. Silva de Cerqueira, M. Hurtado, V. Villegas, V. Granja, M. Villena, R. Vásquez, E. Llop, J. R. Sandoval, A. A. Salazar-Granara, M.-L. Parolin, K. Sandoval, R. I. Peñaloza-Espinosa, H. Rangel-Villalobos, C. A. Winkler, W. Klitz, C. Bravi, J. Molina, D. Corach, R. Barrantes, V. Gomes, C. Resende, L. Gusmão, A. Amorim, Y. Xue, J.-M. Dugoujon, P. Moral, R. González-José, L. Schuler-Faccini, F. M. Salzano, M.-C. Bortolini, S. Canizales-Quinteros, G. Poletti, C. Gallo, G. Bedoya, F. Rothhammer, D. Balding, G. Hellenthal, and A. Ruiz-Linares, "Latin Americans show wide-spread Converso ancestry and imprint of local Native ancestry on physical appearance," Nat. Commun. **9**(1), 5388 (2018).
54. N. G. Crawford, D. E. Kelly, M. E. B. Hansen, M. H. Beltrame, S. Fan, S. L. Bowman, E. Jewett, A. Ranciaro, S. Thompson, Y. Lo, S. P. Pfeifer, J. D. Jensen, M. C. Campbell, W. Beggs, F. Hormozdiari, S. W. Mpoloka, G. G. Mokone, T. Nyambo, D. W. Meskel, G. Belay, J. Haut, H. Rothschild, L. Zon, Y. Zhou, M. A. Kovacs, M. Xu, T. Zhang, K. Bishop, J. Sinclair, C. Rivas, E. Elliot, J. Choi, S. A. Li, B. Hicks, S. Burgess, C. Abnet, D. E. Watkins-Chow, E. Oceana, Y. S. Song, E. Eskin, K. M. Brown, M. S. Marks, S. K. Loftus, W. J. Pavan, M. Yeager, S. Chanock, S. A. Tishkoff, and S. A. Tishkoff; NISC Comparative Sequencing Program, "Loci associated with skin pigmentation identified in African populations," Science **358**(6365), eaan8433 (2017).
55. J. Y. Suen, P. Tewari, Z. D. Taylor, W. S. Grundfest, H. Lee, E. R. Brown, M. O. Culjat, and R. S. Singh, "Towards medical terahertz sensing of skin hydration," Stud. Health Technol. Inform. **142**, 364–368 (2009).
56. N. Bajwa, S. Sung, D. B. Ennis, M. C. Fishbein, B. N. Nowroozi, D. Ruan, A. Maccabi, J. Alger, M. A. S. John, W. S. Grundfest, and Z. D. Taylor, "Terahertz Imaging of Cutaneous Edema: Correlation With Magnetic Resonance Imaging in Burn Wounds," IEEE Trans. Biomed. Eng. **64**(11), 2682–2694 (2017).